Bioorganic & Medicinal Chemistry Letters 19 (2009) 2230–2234

Contents lists available at ScienceDirect

Bioorganic & Medicinal Chemistry Letters

journal homepage: www.elsevier.com/locate/bmcl

1-Aryl-3,4-dihydroisoquinoline inhibitors of JNK3

John A. Christopher [a,*], Francis L. Atkinson [b], Benjamin D. Bax [b], Murray J. B. Brown [b], Aurélie C. Champigny [a], Tsu Tshen Chuang [b], Emma J. Jones [b], Julie E. Mosley [b], James R. Musgrave [b,†]

[a] GlaxoSmithKline R&D, Medicines Research Centre, Gunnels Wood Road, Stevenage, Hertfordshire SG1 2NY, UK
[b] GlaxoSmithKline R&D, New Frontiers Science Park, Third Avenue, Harlow, Essex CM19 5AW, UK

ARTICLE INFO

Article history:
Received 28 December 2008
Revised 24 February 2009
Accepted 25 February 2009
Available online 28 February 2009

Keywords:
Kinase
Inhibitor
JNK
JNK3
MAPK
Selective

ABSTRACT

A series of 1-aryl-3,4-dihydroisoquinoline inhibitors of JNK3 are described. Compounds **20** and **24** are the most potent inhibitors (pIC50 7.3 and 6.9, respectively in a radiometric filter binding assay), with 10- and 1000-fold selectivity over JNK2 and JNK1, respectively, and selectivity within the wider mitogen-activated protein kinase (MAPK) family against p38α and ERK2. X-ray crystallography of **16** reveals a highly unusual binding mode where an H-bond acceptor interaction with the hinge region is made by a chloro substituent.

Protein kinases catalyse the phosphorylation of tyrosine and serine/threonine residues in proteins involved in the regulation of diverse cellular functions. Aberrant kinase activity is implicated in many diseases, which makes the inhibition of kinases an attractive target for the pharmaceutical industry.[1]

The mitogen-activated protein kinase (MAPK) pathways comprise a major signaling system used to transduce extracellular signals to intracellular responses. The MAPK family of serine-threonine protein kinases consists of the extracellular-regulated protein kinases (ERK), p38 mitogen-activated kinases (p38 MAPK) and the c-Jun N-terminal kinases (JNKs).[2]

c-Jun N-terminal kinases are implicated in several disease areas, including neurodegeneration, rheumatoid arthritis, inflammatory disorders, cancer and diabetes.[3,4] They differ in their tissue expression profile and functions, with JNK1 and JNK2 being widely expressed, whereas JNK3 is expressed predominantly in the brain and at lower levels in the heart and testes.[5,6] JNK3 appears to play important roles in the brain to mediate neurodegeneration, such as beta amyloid processing, Tau phosphorylation and neuronal apoptosis in Alzheimer's Disease, as well as the mediation of neurotoxicity in a rodent model of Parkinson's Disease.[7–9] Identifying potent inhibitors of JNK3, with selectivity within the wider MAPK family, may contribute towards neuroprotection therapies with reduced side effect risks and will aid the further understanding of the roles of the individual JNK kinases. Only a few cases of inhibitors with significant selectivity within the JNK family have been published, recent examples being **1**–**3**, Table 1.[10–12] JNK inhibitors have been recently reviewed.[13]

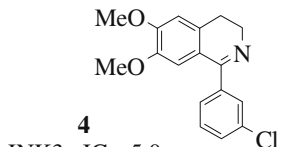

4
JNK3 pIC_{50} 5.0

A screening exercise to identify new JNK3 inhibitors identified dihydroisoquinoline **4** as a weakly potent (pIC_{50} 5.0) inhibitor.

Searching of the GlaxoSmithKline corporate collection identified numerous closely related analogues. A selection was screened in JNK3 and p38α fluorescence anisotropy kinase binding assays; data are summarised in Table 2.[14,15]

This initial iteration of analog screening revealed several interesting aspects to the series. Firstly, numerous changes to R^1 with methoxy R^6 and R^7 groups failed to increase JNK3 potency; at best the moderate activity of the initial hit **4** was retained. Changes to the R^6 and R^7 positions had a moderate impact; compounds **11** and **13** where the 7-position methoxy group was replaced by chloro yielded slight increases in JNK3 inhibitory activity over the initial hit, albeit with different R^1 substituents to **4**. Interestingly, the analogues where the positions of the methoxy and chloro

* Corresponding author. Tel.: +44 0 1438 763578.
E-mail address: john@christopher257.fsnet.co.uk (J.A. Christopher).
† Present address: Medimmune Cambridge, Milstein Building, Granta Park, Cambridge, CB21 6GH, UK.

0960-894X/$ - see front matter © 2009 Elsevier Ltd. All rights reserved.
doi:10.1016/j.bmcl.2009.02.098

Table 1
Selective JNK inhibitors **1**–**3**, values in pIC_{50}

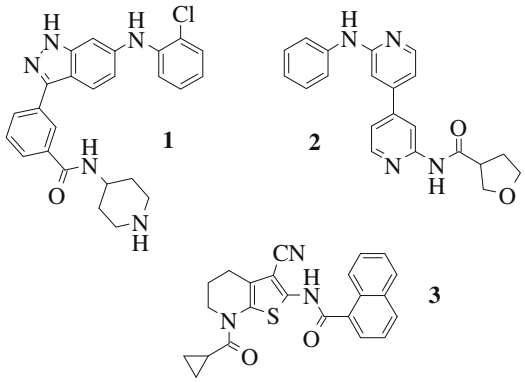

Compound	JNK1	JNK2	JNK3	p38α	Erk-2
1[10]	7.1	*NR*	8.9	8.4	NR
2[11]	6.4	*NR*	8.2	6.7	NR
3[12]	<5.0	6.5	6.6	<4.8	<5.0

NR: Not reported.

substituents are interchanged were inactive at JNK3 (compare **11** with **12**, **13** with **14**). No inhibition of p38α was observed.

Encouraged by the moderate JNK3 activity and the initial indications of selectivity within the MAPK family, representative molecules such as **11** were docked into the active site of JNK3, Figure 1.[16] Analysis of the dockings suggested the conserved hydrogen-bond from the hinge backbone amide (Met149 in JNK3) was accepted by the dihydroisoquinoline nitrogen, with the R^1 aromatic substituent occupying the outer lipophilic region.[19] This motif is reminiscent of that seen in the crystal structure of close analogues of **1**, where the conserved H-bond is accepted by the indazole N2.[10] By contrast, in the dihydroisoquinoline dockings the inner H-bond to the backbone carbonyl (Glu147 in JNK3) is lost, whereas in **1** it is donated by the indazole N1. However, this donor interaction, whilst common, is by no means entirely conserved, and the absence was not taken to contradict the binding mode hypothesis. The substituents at R^6 and R^7 make few interactions with the site, which suggested that there might be significant opportunities for improving this template.

With this binding hypothesis in hand, we initiated an exploration of the template to understand the profile of the molecules

Table 2
JNK3 and p38α inhibition (fluorescence anisotropy kinase binding assay) of compounds **5**–**14**, values in pIC_{50}

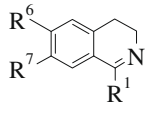

Compound	R^1	R^6	R^7	JNK3	p38α
5	3,4-Cl_2-Phenyl	OMe	OMe	5.2	<4.8
6	Phenyl	OMe	OMe	<4.8	<4.8[a]
7	4-Cl-Phenyl	OMe	OMe	<4.8	<4.8
8	3-MeO-Phenyl	OMe	OMe	<4.8	<4.8
9	3-Cl-Phenyl	Cl	OMe	4.9	<4.8[a]
10	3-Cl-Phenyl	H	H	<4.8	<4.8
11	3-F-Phenyl	OMe	Cl	5.4	<4.8
12	3-F-Phenyl	Cl	OMe	<4.8	<4.8[a]
13	4-F-Phenyl	OMe	Cl	5.3	<4.8
14	4-F-Phenyl	Cl	OMe	<4.8	<4.8[a]

[a] TR-FRET data.[15]

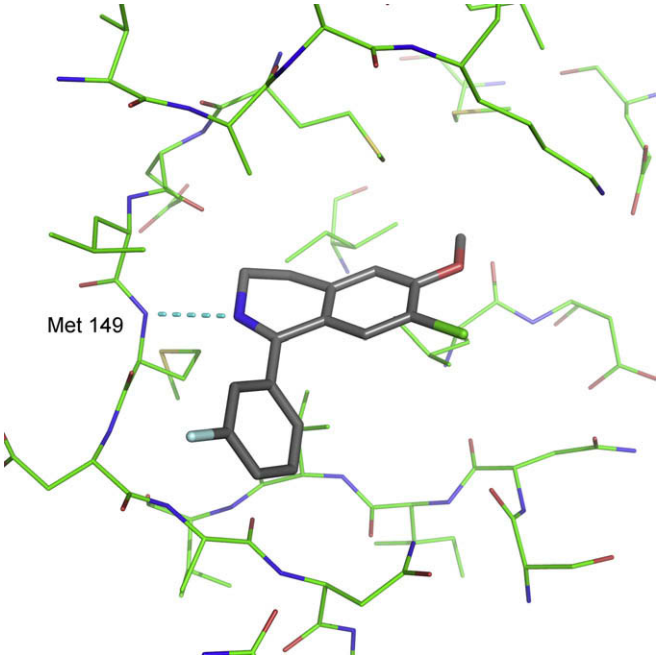

Figure 1. Compound **11** docked into the active site of JNK3.[16]

within the wider JNK family, with the aim of improving the JNK3 potency and gaining a clearer understanding of the structure–activity relationships. Screening of further analogs of the series from the GlaxoSmithKline corporate collection was complemented by synthesis of key molecules, focusing on the R^6 and R^7 positions.

The synthetic route was straightforward; appropriately substituted phenylethylamines **15** were acylated and then cyclised with phosphorous oxychloride, as depicted in Scheme 1. Data for representative compounds from this exercise are summarized in Table 3. The most active JNK3 inhibitors were those bearing methoxy substitution at R^6 and chloro substitution at R^7, analogues where these two substituents were interchanged were at best weakly active at JNK3 (compare **16**, **20**, and **24** with **17**, **21** and **9** (Table 2), respectively). Gratifyingly, selectivity over p38α was maintained. Mono- or di-substituted phenyl groups at R^1 were preferred for JNK3, amongst the most active being *meta*-bromo or chloro compounds **16** and **24**. Comparison of these with the unsubstituted analogue **22** or the *meta*-fluoro variant **11** indicated that the bulk and lipophilicity imparted by the larger halogens provided favourable interactions in the JNK3 ATP binding active site. Other R^1 groups, for example benzyl or alkyl, (**27**, **28**) were not tolerated.

JNK1, JNK2 and JNK3 inhibitory activities of key compounds **20** and **24** were assessed in analogous radiometric filter binding assays, Table 4.[20] Erk-2 data were also obtained, which together with the p38α data already in hand from a fluorescence anisotropy binding assay provides a full picture of selectivity within the wider MAPK family.[20] The data revealed a highly encouraging selectivity profile; **20** and **24** have approximately 10 and 1000-fold selectivity for JNK3 over JNK2 and JNK1, respectively. The JNK family selectiv-

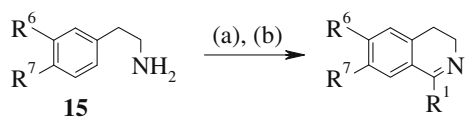

Scheme 1. Synthesis of dihydroisoquinolines. Reagents and conditions: (a) R^1-COCl, CH_2Cl_2, 5% (aq) NaOH, rt; (b) $POCl_3$, CH_2Cl_2, reflux, or microwave heating, 120 °C.

Table 3
JNK3 and p38α inhibition (fluorescence anisotropy kinase binding assay) of compounds **16–28**, values in pIC_{50}

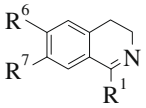

Compound	R^1	R^6	R^7	JNK3	p38α
16	3-Br-Phenyl	OMe	Cl	6.4	4.9
17	3-Br-Phenyl	Cl	OMe	5.0	<4.8[a]
18	2-Napthyl	OMe	Cl	6.0	<4.8
19	2-Napthyl	Cl	OMe	<4.8	<4.8[a]
20	3,4-Cl_2Phenyl	OMe	Cl	6.5	5.1
21	3,4-Cl_2Phenyl	Cl	OMe	4.8	<4.8[a]
22	Phenyl	OMe	Cl	5.2	<4.8
23	Phenyl	Cl	OMe	<4.8	<4.8[a]
24	3-Cl-Phenyl	OMe	Cl	6.6	5.1
25	3-Me-Phenyl	OMe	Cl	5.7	<4.8
26	2-F,3-Cl-Phenyl	OMe	Cl	6.2	4.9
27	-CH_2Phenyl	OMe	Cl	<4.8	<4.8
28	Ethyl	OMe	Cl	<4.8	<4.8

[a] TR-FRET data.[15]

Table 4
JNK1, JNK2, JNK3, Erk-2 and p38α inhibition of compounds **20** and **24**, values in pIC_{50}

Compound	JNK1[a]	JNK2[a]	JNK3[a]	Erk-2[a]	p38α[b]
20	4.0	6.1	7.3	<4.0	5.1
24	<4.0	5.9	6.9	<4.0	5.1

[a] Radiometric filter binding assay.[20]
[b] Fluorescence anisotropy kinase binding assay.[15]

ity is complemented by selectivity within the wider MAPK family over Erk-2 and p38α, approximately 1000- and 100-fold, respectively.

The MAPK selectivity of the template is matched by an encouraging wider selectivity profile. For example **20** and **24** were inactive ($pIC_{50} < 5.0$) at numerous kinases, including B-Raf, c-Fms, CDK-2, EGFR, ErbB2, GSK3β, IKK-α, IKK-β, Lck, MLK3, PLK1, Rock1 and SGK1.

Intrigued by the clear SAR trends that had emerged, we sought to obtain a ligand-bound crystal structure to aid our understanding. A crystal structure of compound **16** complexed with JNK3 was obtained to 2.4 Å resolution, which revealed a binding mode very different to that expected from the docking experiments (Fig. 2).[21]

Firstly, contact with the hinge is made by the chloro(methoxy)benzene moiety, not by the dihydroisoquinoline nitrogen. Secondly, the R^1 aromatic substituent occupies an 'induced-fit' hydrophobic pocket at the rear of the active site, not the outer lipophilic region.

The conserved hydrogen-bond with the hinge donor (the backbone NH of Met149) appears to be made by the R^7 chlorine atom.[19] Such hydrogen bonds with organic halogens as acceptors are rare: however, recent studies utilizing small-molecule crystal-structure database surveys or ab initio calculations have shown that such interactions are genuine, if weaker than 'normal' H-bonds to oxygen or nitrogen acceptors.[22–24] These interactions have not yet been systematically studied in protein–ligand crystal structures, but have been shown to occur in the PDB.[25] The Cl···H distance here is 2.7 Å, the Cl···H–N angle 127° and the H···Cl–C angle 113°.[26] These parameters are consistent with those observed in the small-molecule database studies, placing the interaction towards the weaker end of the scale in the classification of Jeffrey.[22,23,27]

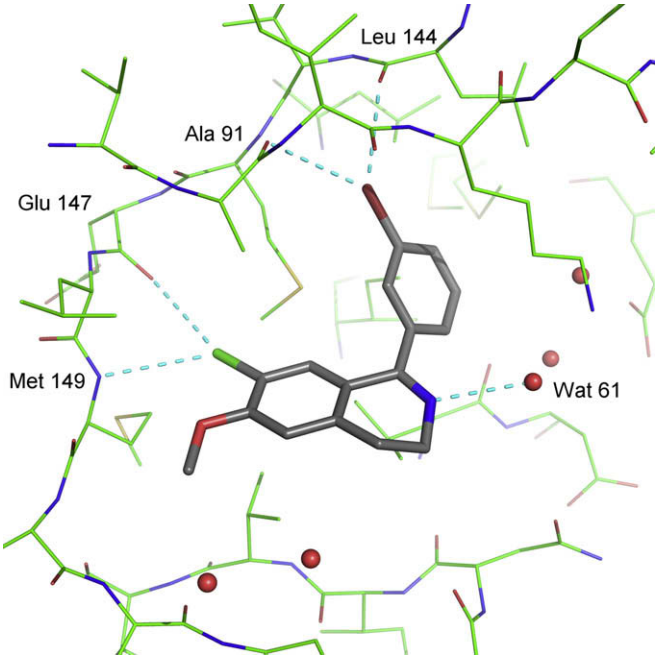

Figure 2. Crystal structure of compound **16** in the JNK3 active site.[21]

A second interaction made by the chlorine is a contact (3.4 Å) with the backbone carbonyl of Glu147; this 'inner' carbonyl accepts an H-bond from ATP and is commonly utilized by kinase inhibitors.[17,19] Attractive interactions between halogens, here acting as a Lewis acid, and Lewis bases such as oxygen are termed 'halogen bonds'; they are less well known than hydrogen bonds, but have attracted considerable attention in recent years. Small-molecule crystal-structure database surveys, ab initio calculations and gas-phase studies have shown beyond doubt that such interactions can be attractive and of non-negligible strength.[28–32] In addition, recent studies have shown that such interactions occur in protein–ligand crystal structures.[32,33]

In the present structure the C–Cl···O angle is 163°, which is consistent with the literature data showing that, in a halogen bond, a linear geometry is preferred about the halogen atom.[28–30] Calculations show that the electron density around the halogen is anisotropic, meaning the halogen atom has a 'crown' of positive electrostatic potential in the direction of the C–Hal bond, surrounded by a band of negative electrostatic potential.[24,32,34,35] The positive crown is responsible for 'head-on' interactions with electron donors (i.e., halogen bonds), the negative band for 'side-on' interactions with proton donors (i.e., hydrogen bonds).[22,23,25,36] The polar interactions of the chlorine in this structure illustrate this 'amphiphilic' nature of halogens, a property that has also been observed in molecular crystals.[24,37]

The C=O···Cl angle observed here is 139°, and inspection shows that the chlorine lies close to the plane of the carbonyl. Both these observations are consistent with the interaction being with an oxygen lone pair; it should be noted that this preference is not necessarily very strong.[28]

Whilst the polar interactions of the R^7 chloro substituent with the hinge region described above are interesting, the question of how much they actually contribute to binding remains open. It is likely that binding is driven primarily by contacts with hydrophobic residues (discussed further below), and it might be that the contribution of the polar interactions made by the chlorine to the affinity is minor. However, a precedent for the halogen-mediated interaction of **16** with the hinge can be seen in the complex of 4,5,6,7-tetrabromobenzotriazole **29** with CDK2 (PDB 1P5E).[36] Here,

the bromine in the 5-position makes a halogen bond with the carbonyl oxygen of Glu81, which corresponds to Glu147 of JNK3. This bromine also contacts the conserved donor residue in CDK2 (the backbone NH of Leu83); although the geometry is poor, this might constitute a weak H-bond, similar to that seen with **16**.

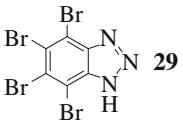

29

Replacement of the R^7 chlorine of **16** with bromine, fluorine or other groups capable of accepting a hydrogen bond are outside the scope of this communication, but would serve to further probe the importance for inhibition of this substituent.

The methoxy substituent at R^6 impinges on the outer lipophilic region, and makes contacts with hydrophobic residues there (e.g., Ile70, Leu148 and Ala151).[19] Further, it might modulate the electron density on the chlorobenzene moiety, and thus affect the polar interactions discussed above. However, the lack of SAR around this position means these effects require further study.

The isoquinoline moiety occupies the adenine-binding region, and makes extensive contacts with the hydrophobic residues surrounding it (e.g., Ile70, Val78, Ala91, Met 146, Val196, and Leu206).[19] Additionally, the isoquinoline nitrogen accepts a hydrogen-bond from a water molecule that is also H-bonded to the conserved Lysine (Lys93).

The R^1 substituent of **16** occupies a lipophilic pocket at the back of the active site that is exposed by the rearrangement of the gatekeeper residue Met146 and is formed mainly by the sidechains of Met146, Ala91, Leu144, Ile124, Leu206 and Lys93 (the lipophilic portion thereof).[10–12]

In addition to these non-polar contacts, the bromine atom of **16** is in contact with the backbone carbonyl oxygens of Leu144 (3.1 Å) and Ala91 (3.3 Å). These interactions appear to be further examples of the halogen bond; in contrast to the situation described above, however, the halogen in both these cases lies approximately perpendicular to the carbonyl plane, suggesting that the interaction is with the π-electrons of the peptide bond instead of with an oxygen lone pair.[32]

The importance of these halogen bonds can perhaps be gauged by comparison of the JNK3 potency of compound **16** with that of **25** (Table 3). In the latter the bromine is replaced by a methyl group, and the potency is reduced by ~0.7 log units. In addition, the chloro-analogue of **16** (compound **24**), which can also presumably make the halogen bonds seen in the crystal structure, shows activity almost a log unit better than **25**. If the role of the halogen or methyl in these compounds was purely to enhance the steric complementarity of the R^1 substituent to the hydrophobic pocket then this difference might not be expected.

The induced-fit pocket contains the only active-site residue that differs between JNK3 and JNK1, Leu144 in the former corresponding to Ile106 in the latter. In common with the rationale postulated for **3** we believe that the significant selectivity exhibited by this series for JNK3 over JNK1 could result from the difference in the shape of the hydrophobic pocket introduced by this change.[12]

This selectivity rationale assumes that the binding mode observed in JNK3 is conserved in JNK1. Despite the relatively low affinity of these compounds for JNK1 (Table 4), it proved possible to obtain protein–ligand crystal structures of **24** and **26** complexed with JNK1, which both showed the same binding mode as **16** in JNK3.[21]

Only one residue differs in the active sites of JNK3 and JNK2; Met115 in the former corresponding to Leu77 in the latter. The series has only moderate selectivity for JNK3 over JNK2, indicative of the fact that this residue is peripheral, and thus would not be expected to significantly impact inhibitor binding.

The residues that comprise the induced-fit pocket in JNK3 are largely conserved in p38α, a notable exception being the gatekeeper, which is Thr106 in p38α. Despite these similarities, inspection of the structures of JNK3 with **16** and of comparable p38α crystal structures suggests that there are considerable differences in the shape of the pocket, due to, for example, differences in domain orientation.[38] This, alongside the differing gatekeeper and differences in the hinge region, means the lack of p38α activity can be easily understood.

The gatekeeper residue in Erk-2 is Gln103, which does not undergo the rearrangement observed for Met146 in JNK3, and this kinase is believed to be relatively insensitive to back-pocket binding ligands.[39] The lack of Erk-2 inhibitory activity of **20** and **24** was thus expected.

In summary, 1-aryl-3,4-dihydroisoquinolines such as **20** and **24** represent a potent series of JNK3 inhibitors (pIC_{50} 7.3 and 6.9, respectively in a radiometric filter binding assay), with 10- and 1000-fold selectivity over JNK2 and JNK1, respectively, and an encouraging wider kinase selectivity profile. The highly unusual binding mode where the conserved H-bond acceptor interaction with the hinge region is made by the R^7 chloro substituent is a key feature of the series, and with this structural information in hand, optimization of the R^1 and R^6 substituents is a focus for future investigations.

Acknowledgments

Yvonne Joseph, Jeffery Smith, Laurie Gordon and the GSK Screening and Compound Profiling group are gratefully acknowledged for the generation of kinase inhibition data. Synthetic contributions from K. Franzmann, F. Copp, S. Swanson and C. Foster are gratefully acknowledged.

References and notes

1. Parang, K.; Sun, G. *Curr. Opin. Drug Disc. Dev.* **2004**, *7*, 617.
2. Herlaar, E.; Brown, Z. *Mol. Med. Today* **1999**, *5*, 439.
3. Manning, A. M.; Davis, R. J. *Nat. Rev. Drug Disc.* **2003**, *2*, 554.
4. Liu, G.; Rondinone, C. M. *Curr. Opin. Invest. Drugs* **2005**, *6*, 979.
5. Kuan, C.-Y.; Yang, D. D.; Roy, D. R. S.; Davis, R. J.; Rakic, P.; Flavell, R. A. *Neuron* **1999**, *22*, 667.
6. Martin, J. H.; Mohit, A. A.; Miller, C. A. *Mol. Brain Res.* **1996**, *35*, 47.
7. Resnick, L.; Fennell, M. *Drug Discovery Today* **2004**, *9*, 932.
8. Kimberley, W. T.; Zheng, J. B.; Town, T.; Flavell, R. A.; Selkoe, D. J. *J. Neurosci.* **2005**, *25*, 5533.
9. Pan, J.; Wang, G.; Yang, H.-Q.; Hong, Z.; Xiao, Q.; Ren, R.-J.; Zhou, H.-Y.; Bai, L.; Chen, S.-D. *Mol. Pharmacol.* **2007**, *72*, 1607.
10. Swahn, B.-M.; Huerta, F.; Kallin, E.; Malmström, J.; Weigelt, T.; Viklund, J.; Womack, P.; Xue, Y.; Öhberg, L. *Bioorg. Med. Chem. Lett.* **2005**, *15*, 5095.
11. Swahn, B.-M.; Xue, Y.; Arzel, E.; Kallin, E.; Magnus, A.; Plobeck, N.; Viklund, J. *Bioorg. Med. Chem. Lett.* **2006**, *16*, 1397.
12. Angell, R. M.; Atkinson, F. L.; Brown, M. J.; Chuang, T. T.; Christopher, J. A.; Cichy-Knight, M.; Dunn, A. K.; Hightower, K. E.; Malkakorpi, S.; Musgrave, J. R.; Neu, M.; Rowland, P.; Shea, R. L.; Smith, J. L.; Somers, D. O.; Thomas, S. A.; Thompson, G.; Wang, R. *Bioorg. Med. Chem. Lett.* **2007**, *17*, 1296.
13. LoGrasso, P.; Kamenecka, T. *Mini-Rev. Med. Chem.* **2008**, *8*, 755.
14. $pIC_{50} = -Log_{10}\ IC_{50}$; where the IC_{50} is the concentration of compound required to inhibit the kinase activity by 50%. JNK3 inhibitory activity was determined using a fluorescence anisotropy kinase binding assay. The kinase, a fluorescently labeled inhibitor and a variable concentration of test compound are incubated together to reach thermodynamic equilibrium under conditions such that in the absence of test compound the fluorescent inhibitor is significantly (>50%) enzyme bound and in the presence of a sufficient concentration ($>10 \times K_i$, where K_i = dissociation constant for inhibitor binding) of a potent inhibitor the anisotropy of the unbound fluorescent ligand is measurably different from the bound value. Truncated human JNK3 was expressed in baculovirus as an N-terminal His (6)-tagged fusion protein. This enzyme (JNK3) was activated in 50 mM Tris/HCl pH 7.5, 0.1 mM EGTA, 0.1% beta-mercaptoethanol, 0.1 mM sodium vanadate, 10 mM magnesium acetate, 0.1 mM ATP with 100 nM active MKK4 and MKK7beta at 30 °C for 30 min. Following activation, the JNK3 is purified by Ni-NTA agarose chromatography. The JNK3 was then dialyzed into storage buffer (50 mM Tris/HCl pH 7.5, 270 mM Sucrose, 150 mM NaCl, 0.1 mM EGTA, 0.1% beta-

mercaptoethanol, 0.03% Brij-35, 1 mM benzamidine, 0.2 mM PMSF), snap frozen in liquid nitrogen and stored at −70 °C. Inhibitor binding to JNK3 was assessed by a fluorescence anisotropy competitive binding assay. All components are dissolved in buffer of composition 50 mM HEPES, pH 7.5, 1 mM CHAPS, 1 mM DTT, 10 mM $MgCl_2$ with final concentrations of 10 nM JNK3 and 2 nM of a fluorescently labeled inhibitor. This reaction mixture is added to wells containing various concentrations of test compound (0.28 nM–16.6 μM final) or DMSO vehicle (<3% final) in black 384-well microtitre plates and equilibrated for 30–300 min at room temperature to reach equilibrium. Fluorescence anisotropy is read in Molecular Devices Acquest (excitation 530 nm/emission 580 nm). The error of the assay is estimated as ±0.2 log units, based on the median standard deviation of all compounds which have been tested more than eight times and have a mean $pIC_{50} > 6$.

15. p38α Fluorescence anisotropy kinase binding assay data were generated using conditions previously described, see: Barker, M. D.; Hamblin, J. N.; Jones, K. L.; Patel, V. K.; Swanson, S.; Walker, A. L. Int. Patent Appl. WO 05/073232. Alternatively, where indicated, p38α inhibitory activity was determined using a time-resolved fluorescence resonance energy transfer (TR-FRET) assay: Recombinant His-tagged human p38α was activated using 3 μM unactivated p38α incubated in 200 mM Hepes pH 7.4, 625 mM NaCl; 1 mM DTT with 27 nM active MKK6 (Upstate). Biotinylated GST-ATF2 (residues 19–96, 400 nM final), ATP (125 mM final) and $MgCl_2$ (5 mM final) in assay buffer (40 mM HEPES pH 7.4, 1 mM DTT) were added to wells containing 1 μl of various concentrations of compound or DMSO vehicle (3% final) in NUNC 384-well black plates. The reaction was initiated by addition of p38α (100 pM final) to give a total volume of 30 μl. After 120 min incubation (rt), 15 μl of 100 mM EDTA pH 7.4 was added followed by detection reagent (15 μl) in buffer (100 mM HEPES pH 7.4, 150 mM NaCl, 0.1% w/v/BSA, 1 mM DTT) containing antiphosphothreonine-ATF2-71 polyclonal antibody (Cell Signalling Technology, Beverly Massachusetts, MA) labelled with W-1024 Eu chelate (Wallac OY, Turku, Finland), and APC-labelled streptavidin (Prozyme, San Leandro, CA). After 60 min further incubation (rt) the ATF-2 phosphorylation was measured using a Packard Discovery plate reader (Perkin–Elmer, Pangbourne, UK) as a ratio of specific 665 nm energy transfer signal to reference Eu 620 nm signal.
16. The public-domain JNK3 crystal structure (PDB accession code 1JNK) was used for docking.[17] ATP and water molecules were removed from the PDB file and ligands were docked into the active site using GOLD.[18]
17. Xie, X.; Gu, Y.; Fox, T.; Coll, J. T.; Fleming, M. A.; Markland, W.; Caron, P. R.; Wilson, K. P.; Su, M. S.-S. *Structure* **1998**, *6*, 983.
18. Jones, G.; Willett, P.; Glen, R. C.; Leach, A. R.; Taylor, R. *J. Mol. Biol.* **1997**, *267*, 727.
19. Adams, J. L.; Veal, J.; Shewchuk, L. In *Protein Crystallography in Drug Discovery*; Babine, R. E., Abdel-Meguid, S. S., Eds.; Wiley-VCH: Weinheim, 2004. Chapter 2.
20. Data in radiometric filter binding assays were obtained from Millipore using the IC_{50} Profiler Express™ service, for further details see: www.millipore.com. JNK data were obtained using N-terminal His-tagged full-length human JNK1α1, JNK2α2 or JNK3 with ATF2 as substrate, in the presence of 45, 45, or 10 μM ATP, respectively. Erk-2 data were obtained in a radiometric filter binding assay using N-terminal GST-tagged full-length human Erk-2, activated with MEK1, with myelin basic protein as substrate, in the presence of 155 μM ATP.
21. Truncated JNK3 (Jnk3t; residues 39–402)[14] was purified following a five stage process after lysis of *E. coli* cells expressing GST-JNK3t. [Glutathione Sepharose (GSH), Thrombin cleavage, GSH, Source 15-Q anion exchange, SEC]. The protein was supplied in 50 mM Tris/HCl pH 8.0, 150 mM NaCl post final stage Superdex 200 prep grade Size Exclusion column. Co-crystals of Jnk3t with **16** were grown at 20 °C using the hanging drop method combined with micro-seeding. Protein at 13 mg/mL, pre-incubated with 5 mM compound, was mixed with serial dilutions of a Jnk3t seed stock (made in 25% peg 3350, 0.1 M sodium Hepes pH7.5). Drops were then equilibrated over a reservoir containing 18% peg3350, 0.1 M sodium Hepes pH7.5) before freezing in mother liquor plus 15% glycerol. A 2.4 Å dataset was collected from a single frozen crystal of Jnk3t/**16** on a Mar345 detector mounted on a micromax 007HF rotating anode generator. The crystal structure was refined starting from the coordinates of another Jnk3t complex crystal stucture (pdb code: 2O0U—ligand removed before start of refinement). The deposition code for the Jnk3t/**16** complex is 2waj. Crystal structures of **24** and **26** with a similarly truncated version of Jnk1 are virtually identical (Bax et al., unpublished results).
22. Brammer, L.; Bruton, E. A.; Sherwood, P. *Cryst. Growth Des.* **2001**, *1*, 277.
23. Sony, S. M. M.; Ponnuswamy, M. N. *Bull. Chem. Soc. Jpn.* **2006**, *79*, 1766.
24. Lu, Y.-X.; Zou, J.-W.; Wang, Y.-H.; Zhang, H.-X.; Yu, Q.-S.; Jiang, Y.-J. *J. Mol. Struct.: THEOCHEM* **2006**, *766*, 119.
25. Panigrahi, S. K.; Desiraju, G. R. *Proteins: Struct. Funct. Bioinform.* **2007**, *67*, 128.
26. Note that the hydrogen atoms were not resolved in this structure: where necessary for analysis of the H-bond geometries they were added in standard positions using Maestro (Schrödinger Inc.).
27. *An Introduction to Hydrogen Bonding*; Jeffrey, G. A., Ed.; Oxford University Press: New York, 1997.
28. Lommerse, J. P. M.; Stone, A. J.; Taylor, R.; Allen, F. H. *J. Am. Chem. Soc.* **1996**, *118*, 3108.
29. Ouvrard, C.; Le Questel, J.-Y.; Berthelot, M.; Laurence, C. *Acta Crystallogr., Sect. B* **2003**, *B59*, 512.
30. Legon, A. C. *Angew. Chem., Int. Ed.* **1999**, *38*, 2686.
31. Riley, K. E.; Merz, K. M. *J. Phys. Chem. A* **2007**, *111*, 1688.
32. Auffinger, P.; Hays, F. A.; Westhof, E.; Ho, P. S. *Proc. Natl. Acad. Sci. U.S.A.* **2004**, *101*, 16789.
33. Voth, A. R.; Ho, P. S. *Curr. Top. Med. Chem.* **2007**, *7*, 1336.
34. Bosch, E.; Barnes, C. L. *Cryst. Growth Des.* **2002**, *2*, 299.
35. Clark, T.; Hennemann, M.; Murray, J. S.; Politzer, P. *J. Mol. Model.* **2007**, *13*, 291.
36. PDB accession code 1P5E, see: De Moliner, E.; Brown, N. R.; Johnson, L. N. *Eur. J. Biochem.* **2003**, *270*, 3174.
37. Lieberman, H. F.; Davey, R. J.; Newsham, D. M. T. *Chem. Mater.* **2000**, *12*, 490.
38. Scapin, G.; Patel, S. B.; Lisnock, J.; Becker, J. W.; LoGrasso, P. V. *Chem. Biol.* **2003**, *10*, 705.
39. Wang, Z.; Canagarajah, B. J.; Boehm, J. C.; Kassisà, S.; Cobb, M. H.; Young, P. R.; Abdel-Meguid, S.; Adams, J. L.; Goldsmith, E. J. *Structure* **1998**, *6*, 1117.